Phospholipase C-Mediated Regulation of Transient Receptor Potential Vanilloid 6 Channels: Implications in Active Intestinal Ca^{2+} Transport

Baskaran Thyagarajan, Bryan S. Benn, Sylvia Christakos, and Tibor Rohacs

Department of Pharmacology and Physiology (B.T., T.R.), Department of Biochemistry and Molecular Biology (B.S.B., S.C.), University of Medicine and Dentistry of New Jersey, New Jersey Medical School, Newark, New Jersey

ABSTRACT

Transient receptor potential vanilloid 6 (TRPV6) channels play an important role in intestinal Ca^{2+} transport. These channels undergo Ca^{2+}-induced inactivation. Here we show that Ca^{2+} flowing through these channels activates phospholipase C (PLC) leading to the depletion of phosphatidylinositol 4,5-bisphosphate (PIP$_2$) and formation of inositol 1,4,5-trisphosphate in TRPV6-expressing cells. PIP$_2$ depletion was inhibited by the two structurally different PLC inhibitors 1-[6-[[17β-methoxyestra-1,3,5(10)-trien-17-yl]amino]hexyl]-1H-pyrrole-2,5-dione (U73122) and edelfosine. Ca^{2+}-induced inac-tivation of TRPV6 was also prevented by the PLC inhibitors in whole-cell patch-clamp experiments. Ca^{2+} signals in TRPV6-expressing cells were transient upon restoration of extracellular Ca^{2+} but were rendered more sustained by the PLC inhibitors. Finally, intestinal Ca^{2+} transport in the everted duodenal sac assay was enhanced by edelfosine. These observations suggest that Ca^{2+}-induced inactivation of TRPV6 limits intestinal Ca^{2+} absorption and raise the possibility that Ca^{2+} absorption can be enhanced pharmacologically by interfering with PLC activation.

Intestinal Ca^{2+} absorption is mediated by paracellular (passive) and transcellular (active) mechanisms (Wasserman, 2004). The major regulator of intestinal Ca^{2+} absorption is active vitamin D, 1,25-dihydroxycholecalciferol, which enhances the transcription of several proteins that are important for the transcellular pathway (Christakos et al., 2003). The best characterized of these proteins are TRPV6, the apical Ca^{2+} channel (Peng et al., 1999), and calbindin 9K, a cytoplasmic Ca^{2+} binding protein. Consistent with the role of TRPV6 in active Ca^{2+} absorption, genetic ablation of this gene leads to disturbances in calcium homeostasis, leading to hypocalcemia on a low-calcium diet (Bianco et al., 2006). It is

noteworthy that, on a normal calcium diet, regulatory mechanisms such as increased parathyroid hormone levels can compensate, and the mice have normal serum calcium (Bianco et al., 2006; Benn et al., 2008).

TRPV6 is a member of the transient receptor potential (TRP) ion channel family. TRP channels play a role in a dazzling variety of physiological functions and are activated by a diverse set of stimuli and regulatory pathways (Clapham et al., 2001). Despite their diversity, it seems that these channels may share a common regulatory molecule, phosphatidylinositol 4,5-bisphosphate (PIP$_2$) (Hardie, 2003; Rohacs and Nilius, 2007; Voets and Nilius, 2007). Most TRP channels, including TRPV6 (Thyagarajan et al., 2008) require PIP$_2$ for activity, and loss of this lipid inhibits them (Runnels et al., 2002; Rohacs et al., 2005; Zhang et al., 2005; Nilius et al., 2006).

The closest homolog of TRPV6 is TRPV5, which is mainly expressed in the kidney and plays an important role in calcium reabsorption (Hoenderop et al., 2003, 2005). TRPV5 and TRPV6 are the only Ca^{2+}-selective members of the TRP channel superfamily (den Dekker et al., 2003); most other

ABBREVIATIONS: TRPV6, transient receptor potential vanilloid 6; TRPV5, transient receptor potential vanilloid 5; TRPM8, transient receptor potential melastatin 8; TRPM4, transient receptor potential melastatin 4; PLC, phospholipase C; PIP$_2$, phosphatidylinositol 4,5-bisphosphate; GFP, green fluorescent protein; CFP, cyan fluorescent protein; YFP, yellow fluorescent protein; PH, pleckstrin homology; NDF, nominally divalent-free; FRET, fluorescence resonance energy transfer; IP$_3$, inositol 1,4,5-trisphosphate; U73122, 1-[6-[[17β-methoxyestra-1,3,5-trien-17-yl]amino]hexyl]-1H-pyrrole-2,5-dione; HEK, human embryonic kidney; DMSO, dimethyl sulfoxide; U73343, 1-[6-[[17β-3-methoxyestra-1,3,5-trien-17-yl]amino]hexyl]-2,5-pyrrolidine-dione.

TRP channels are Ca^{2+}-permeable nonselective cation channels (Clapham et al., 2001). Both TRPV6 and TRPV5 are constitutively active and undergo Ca^{2+}-induced inactivation, which is believed to serve as a defense mechanism against Ca^{2+} overload and presumably limits epithelial Ca^{2+} transport (Nilius et al., 2001, 2002). We have shown that Ca^{2+} flowing through TRPV6 induced the depletion of PIP_2, resulting in the inhibition of the channel (Thyagarajan et al., 2008).

In the current study, we focused on the role of PLC in Ca^{2+}-induced PIP_2 depletion and TRPV6 inactivation. We show that Ca^{2+} influx through TRPV6 leads to the depletion of PIP_2 and formation of IP_3, indicating the activation of PLC. Consistent with this, Ca^{2+}-induced PIP_2 depletion was prevented by two structurally different PLC inhibitors, U73122 and edelfosine. The PLC inhibitors also inhibited Ca^{2+}-induced inactivation of TRPV6. Finally, we show that edelfosine increases intestinal Ca^{2+} transport, presumably by inhibiting the inactivation of TRPV6.

Materials and Methods

Cell Culture. HEK293 cells were maintained in minimal essential medium supplemented with 10% fetal bovine serum and penicillin/streptomycin. The human TRPV6 tagged with the *myc* epitope on the N terminus, subcloned into the expression vector pCMV-Tag3A (Stratagene, La Jolla, CA) was used for the experiments (Cui et al., 2002), and cells were transfected using the Effectene reagent. For the intracellular Ca^{2+} imaging and electrophysiology experiments, transfection was confirmed by measuring the fluorescence of cotransfected GFP.

Mammalian Electrophysiology. Whole-cell patch-clamp measurements were performed using a continuous holding protocol at -60 mV, as described earlier (Thyagarajan et al., 2008). Recordings were performed 36 to 72 h after transfection in HEK293 cells using a bath solution containing 137 mM NaCl, 5 mM KCl, 10 mM glucose, and 10 mM HEPES, with pH adjusted to 7.4 (designated as nominally divalent-free, NDF). Note that this solution contains Ca^{2+} in the micromolar range that inhibits TRPV6 channels. Monovalent currents through TRPV6 were initiated using the same solution supplemented with 2 mM EGTA. The same NDF solution was used for the fluorescence measurements and Ca^{2+} imaging. Borosilicate glass pipettes (World Precision Instruments, Sarasota, FL) of 2 to 4 $M\Omega$ resistance were filled with a solution containing 135 mM potassium gluconate, 5 mM KCl, 5 mM EGTA, 1 mM $MgCl_2$, 2 mM ATP disodium, and 10 mM HEPES, pH adjusted to 7.2. The cells were kept in NDF solution for 20 min before measurements. After formation of gigaohm resistance seals, whole-cell configuration was established, and currents were measured using an Axopatch 200B amplifier (Molecular Devices, Sunnyvale, CA). Data were collected and analyzed with the pCLAMP 9.0 Software. All measurements were performed at room temperature (20–25°C).

Fluorescence Resonance Energy Transfer Measurements. HEK293 cells were transfected with the CFP- and YFP-tagged PH domains of PLCδ1 and TRPV6. Measurements were performed using a Photon Technology International (Birmingham, NJ) photomultiplier-based system mounted on an Olympus IX71 microscope (Olympus, Tokyo, Japan) equipped with a Delta-RAM excitation light source. For the fluorescence resonance energy transfer (FRET) measurements, excitation wavelength was 425 nm, and emission was detected parallel at 480 and 535 nm using two interference filters and a dichroic mirror to separate the two emission wavelengths. Data were collected using the Felix software (Photon Technology International), the ratio of traces obtained at the two different wavelengths, correlating with FRET

were plotted (van der Wal et al., 2001). Measurements were performed at room temperature (20–25°C).

Ca^{2+} Imaging. Cells transfected with TRPV6 and GFP (marker for cell selection) were grown on 25-mm circular coverslips and loaded with fura-2 acetoxymethyl ester (2 μM) for 30 to 40 min at room temperature in NDF. The coverslips were then washed in NDF, placed in a stainless steel holder (bath volume, ~0.8 ml; Molecular Probes, Carlsbad, CA), and viewed in a Zeiss Axiovert 100 microscope coupled to an Attofluor digital imaging system (Carl Zeiss Inc., Thornwood, NY). Cells expressing GFP were selected and monitored simultaneously on each coverslip. Results are presented as the ratio (R) of fluorescence intensities at excitation wavelengths of 340 and 380 nm. Cells were continuously superfused with NDF, and Ca^{2+} entry was initiated by the addition of a solution containing 2 mM $CaCl_2$. All experiments were performed at room temperature.

Inositol Phosphate Turnover. Measurements were performed as described by Thyagarajan et al. (2008). HEK293 cells were transfected with TRPV6-myc and incubated with 20 μCi of [*myo*-^{3}H]inositol overnight in growth medium. Before the experiments, the cells were kept in NDF for 20 min and an additional 10 min in NDF containing 10 mM LiCl. Cells were pretreated with U73122 or U73343 for 3 min, followed by a 3-min wash period. Then the cells were treated with NDF containing no Ca^{2+} or 2 mM Ca^{2+} for 25 to 30 min in the continued presence of LiCl. The cells were then scraped, treated with 4% perchloric acid, and centrifuged at 12,000 rpm for 2 to 4 min. The supernatant (1.2 ml) was transferred into glass tubes containing 180 μl of 10 mM EDTA, pH 7.0, and to each tube, 1.3 ml of freshly prepared mixture of trioctylamine/freon mixture was added, vortexed, and centrifuged at 12,000 rpm for 4 min. The top aqueous layer (approximately 1.2 ml) was transferred into plastic vials, and 3.6 ml of sodium bicarbonate was added. This solution was then added to Dowex columns filled with AG1 $\times$ 8 resin (formate form). The columns were then washed 4 times each with 5 ml of distilled water. Fractions 1 to 4 (5 ml each) of 0.4 M ammonium formate/0.1 M formic acid, pH 4.75 (IP_2 fraction), fractions 5 to 8 (5 ml each) of 0.7 M ammonium formate/0.1 M formic acid, pH 4.75 (IP_3 fraction), and fractions 9 to 12 (5 ml each) of 1.2 M ammonium formate/0.1 M formic acid, pH 4.75 (IP_4, IP_5, and IP_6 fraction) were collected. One milliliter of each of the collected fraction was transferred into a scintillation vial, 10 ml of scintillation cocktail was added, and ^{3}H activity was determined in a scintillation counter.

Animals. Male C57BL/6 mice were purchased from Taconic Farms (Albany, NY). Mice were fed a standard rodent chow diet (Rodent Laboratory chow 5001; Ralston Purina Co., St. Louis, MO) ad libitum from birth and were sacrificed at 2 months of age. All of the animal experiments conducted were approved by the University of Medicine and Dentistry of New Jersey Animal Care and Use Committee.

Intestinal Calcium Transport. Intestinal calcium transport was determined by the everted gut sac assay as described earlier (Benn et al., 2008). Everted intestinal sacs were formed from a 5-cm segment of the mouse duodenum proximal to the pyloric junction. A blunt-ended 23-gauge needle was passed into the lumen of the intestinal segment. The distal end of the intestinal segment was then tied to the end of the needle and everted by slowly rolling the proximal end along the needle. The intestinal segment was then filled with 400 μl of transport buffer (125 mM NaCl, 10 mM fructose, 11.3 mM HEPES, and 0.025 mM $CaCl_2$), pH 7.4, at 37°C. The knot of the second ligation was tied, the 23-gauge needle was pulled out, and the everted sacs were preincubated for 20 min in flasks containing 10 ml of preincubation buffer (125 mM NaCl, 10 mM fructose, 11.3 mM HEPES, and 1 mM $CaCl_2$), pH 7.4, at 37°C in the presence of 10 μm of edelfosine or vehicle. After preincubation, the everted sacs were placed in flasks containing 10 ml of transport buffer containing $^{45}CaCl_2$ (20,000 cpm/ml) and 10 μm of edelfosine or vehicle and kept in a water bath at 37°C for 1 h with continuous aeration of 95% O_2/5% CO_2. Time-course studies of calcium transport (30, 60, 90, and 120 min) in our laboratory (author S.C.) indicated a plateau between

90 and 120 min. One hour was chosen as the incubation time because it was in the midpoint of the linear range, allowing for the measurement of increases or decreases in intestinal calcium transport. At the completion of incubation, sacs were removed from the flask, carefully blotted dry, and cut open to collect the internal fluid. The internal fluid and samples from the incubation medium were assayed in triplicate for ^{45}Ca using a scintillation counter. The active accumulation of ^{45}Ca in the inside (serosal) fluid was reported as a ratio of the final concentration of ^{45}Ca inside/outside.

Materials. The PLC inhibitors edelfosine (ET-18-OCH3), U73122 and its inactive analog U73343 were from Axxora (Alexis Laboratories, San Diego, CA). Fura-2 acetoxymethyl ester was obtained from TefLabs (Austin, TX). Effectene was obtained from QIAGEN (Valencia, CA). Cell culture media, antibiotics, and sera were obtained from Invitrogen. All other chemicals were purchased from Sigma (St. Louis, MO).

Data Analysis. Data for all figures were expressed as mean $\pm$ S.E.M. Statistical significance was evaluated by Student's t test.

Results

TRPV6 channels are Ca^{2+}-selective, but in the absence of divalent cations, they also conduct monovalent ions. Monovalent currents are much larger than those carried by Ca^{2+} at physiological Ca^{2+} levels. Most earlier studies examined Ca^{2+}-induced inactivation of TRPV6 at supraphysiological Ca^{2+} concentrations (10–30 mM) and on a relatively short time scale (several hundred milliseconds), initiating Ca^{2+} entry with a negative voltage pulse (Nilius et al., 2002; Derler et al., 2006). We focused on the effects of steady-state Ca^{2+} entry at a constant holding potential on a longer time scale (tens of seconds). We measured monovalent currents through TRPV6 because these can be detected more reliably than the much smaller Ca^{2+} currents in physiological extracellular Ca^{2+} concentrations, as described earlier (Thyagarajan et al., 2008). Figure 1A shows monovalent currents induced by the removal of Ca^{2+} with EGTA at −60 mV. Switching to a solution containing 2 mM Ca^{2+} rapidly inhibits the monovalent current. The second pulse of EGTA induced a smaller current than the first one, reflecting Ca^{2+}-induced inactivation (Thyagarajan et al., 2008). In the control experiments (Fig. 1A), the average current amplitude of the first pulse of 0 Ca^{2+} (1.89 $\pm$ 0.51 nA) was higher than those of the subsequent second (0.77 $\pm$ 0.22 nA) and third (0.61 $\pm$ 0.32 nA) pulses. To examine the role of PLC, we tested the effects of U73122 and its inactive analog U73343.
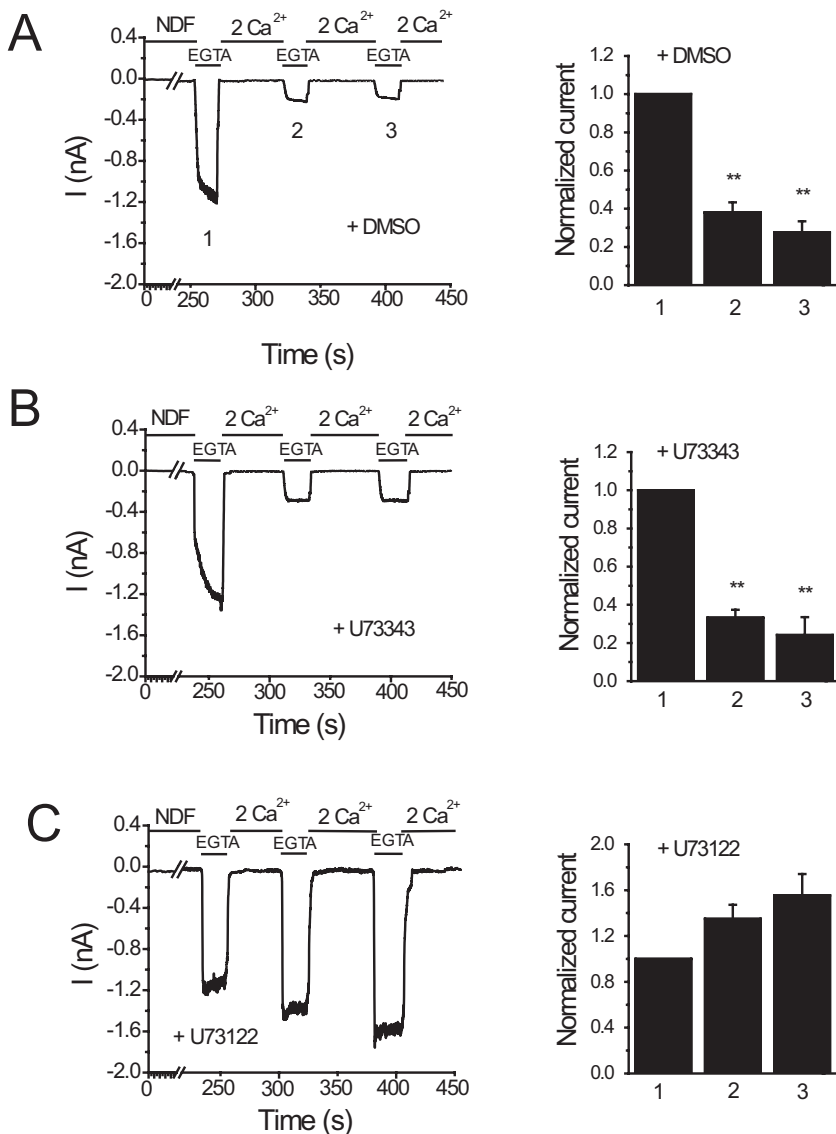

Fig. 1. U73122 inhibits Ca^{2+}-induced inactivation of TRPV6 in patch-clamp experiments. Left, representative whole-cell recordings at a holding potential of −60 mV in HEK293 cells expressing TRPV6. Monovalent currents were initiated by the application of divalent-free solution containing 2 mM EGTA (0 Ca^{2+}) for 20 s followed by application of 2 mM Ca^{2+}. Recordings were performed in cells pretreated with vehicle (DMSO) (A), 3 μM U73343 (B), or 3 μM U73122 (C) for 2 min followed by a 2-min wash. The inhibitors were not present during the measurements. Right, the mean $\pm$ S.E.M. of the currents remaining before the addition of 2 mM Ca^{2+} at time points 1, 2, and 3. The data were normalized to the peak current of the first 0 Ca^{2+} pulse.

For treatment with the inhibitors, we used a protocol similar to that introduced by Horowitz et al. (2005) and was also used by us later (Lukacs et al., 2007). We pretreated the cells with a 3 μM concentration of the inhibitors for 2 min, followed by a 2-min wash, and the inhibitors were not present during the current measurements. This protocol has been shown to minimize the side effects of U73122 (i.e., partial PLC activation) (Horowitz et al., 2005). As shown in Fig. 1B, pretreatment of cells with the inactive U73343, did not prevent Ca^{2+}-induced inactivation of TRPV6 currents. In U73343-treated cells, the maximal amplitude of the current during the first pulse was 1.91 $\pm$ 0.4 nA and during the second and third pulses were 0.61 $\pm$ 0.16 and 0.43 $\pm$ 0.13 nA, respectively. Treatment of cells with the active PLC inhibitor U73122, on the other hand, resulted in relief from Ca^{2+}-induced inactivation (Fig. 1C). The amplitudes of the second (1.26 $\pm$ 0.23 nA) and third pulses (1.37 $\pm$ 0.22 nA) of 0 Ca^{2+} were even higher than that of the first pulse (1.03 $\pm$ 0.21 nA).

Next we tested the effects of U73122 on Ca^{2+} signals elicited by extracellular Ca^{2+} in TRPV6-expressing cells. The cells were loaded with fura-2 in the nominal absence of extracellular Ca^{2+} to remove inactivation. Then extracellular Ca^{2+} was increased from 0 to 2 mM. The cytoplasmic Ca^{2+} signal was transient (Fig. 2A), reflecting Ca^{2+}-induced inactivation of TRPV6 (Derler et al., 2006). When the cells were pretreated with U73122, the Ca^{2+} signal became sustained (Fig. 2C), which is consistent with U73122 inhibiting Ca^{2+}-induced inactivation of TRPV6. U73343 had no effect on the kinetics of Ca^{2+} signal in TRPV6-expressing cells (Fig. 2B).

Next we show that U73122 effectively inhibits PLC activity using two different assays. First, we used a FRET-based assay that monitors translocation of the PH domain of PLCδ1 from the plasma membrane to the cytoplasm (van der Wal et al., 2001; Rohacs et al., 2005). The CFP- and YFP-tagged PH domains bind to PIP_2 and thus are located at the plasma membrane. Upon hydrolysis of the lipid, they translocate to the cytoplasm, which is detected as a decrease in FRET between the CFP- and YFP-tagged PH domains. This is reflected as a downward deflection in the curves in Fig. 3. Increasing extracellular calcium from nominally 0 to 2 mM induced a marked decrease in FRET in TRPV6-expressing cells (Fig. 3A), and this was inhibited by U73122 (Fig. 3C) but not by U73343 (Fig. 3B). This assay measures the depletion of PIP_2, which may happen through the activation of PLC or via dephosphorylation by phosphatases (Suh et al., 2006; Varnai et al., 2006). It has to be noted that the PH domain of PLCδ1 also binds to IP_3, and there is a debate in the literature as to whether the translocation of this construct is mainly caused by the depletion of PIP_2 (van der Wal et al., 2001) or by its displacement as a result of increased IP_3 levels upon PLC activation (Hirose et al., 1999). We have also measured IP_3 formation in response to Ca^{2+} in [^{3}H]inositol-loaded cells (Fig. 3E). U73122, but not U73343, inhibited the IP_3 formation induced by Ca^{2+} in TRPV6-expressing cells.

Next, we tested the effects of another structurally different PLC inhibitor, edelfosine (Horowitz et al., 2005). Figure 4, A and B, shows that edelfosine, similar to U73122, inhibited Ca^{2+}-induced inactivation of TRPV6 currents. In controls, the current amplitude of the first pulse was 2.02 $\pm$ 0.20 nA, the second was 0.46 $\pm$ 0.063 nA, and the third pulse was 0.44 $\pm$ 0.065 nA. In edelfosine-treated cells, the amplitudes of the first, second, and third pulses were 1.64 $\pm$ 0.278, 1.82 $\pm$ 0.212, and 1.8 $\pm$ 0.226 nA, respectively. Edelfosine also rendered Ca^{2+} signals more sustained in TRPV6-expressing cells (Fig. 4C). Figure 5 shows that edelfosine inhibited Ca^{2+}-induced PIP_2 hydrolysis, as indicated by the translocation of the PLCδ1 PH domain measured by the FRET-based assay. We also attempted to use a third PLC inhibitor, neomycin, but it inhibited the peak current amplitude of TRPV6 by ~90% (data not shown); thus, we could not assess its effect on Ca^{2+}-induced inactivation.

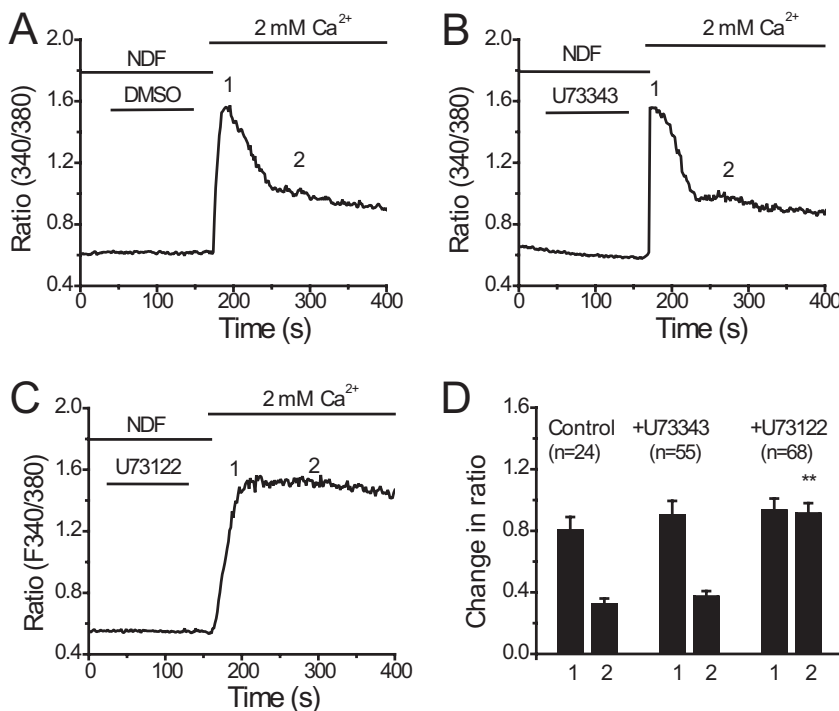The Ca^{2+}-induced inactivation of TRPV6 presumably lim-

Fig. 2. U73122 promotes Ca^{2+} entry into TRPV6-expressing cells. A to C, time courses of increase in fura-2 fluorescence ratio in cells treated with DMSO, U73343 (3 μM), and U73122 (3 μM), respectively. D, the average changes in fluorescence ratio $\pm$ S.E.M. for the peak and 200 s after the addition of extracellular Ca^{2+} in cells treated with DMSO ($n = 24$), U73343 ($n = 55$), or U73122 ($n = 68$).

its intestinal Ca^{2+} transport. To test this assumption and to test the involvement of PLC, we have examined the effect of inhibiting PLC on intestinal Ca^{2+} transport using the everted duodenal gut sac method (Benn et al., 2008). Figure 6 shows that edelfosine significantly enhanced Ca^{2+} transport in the everted duodenal sac assay.
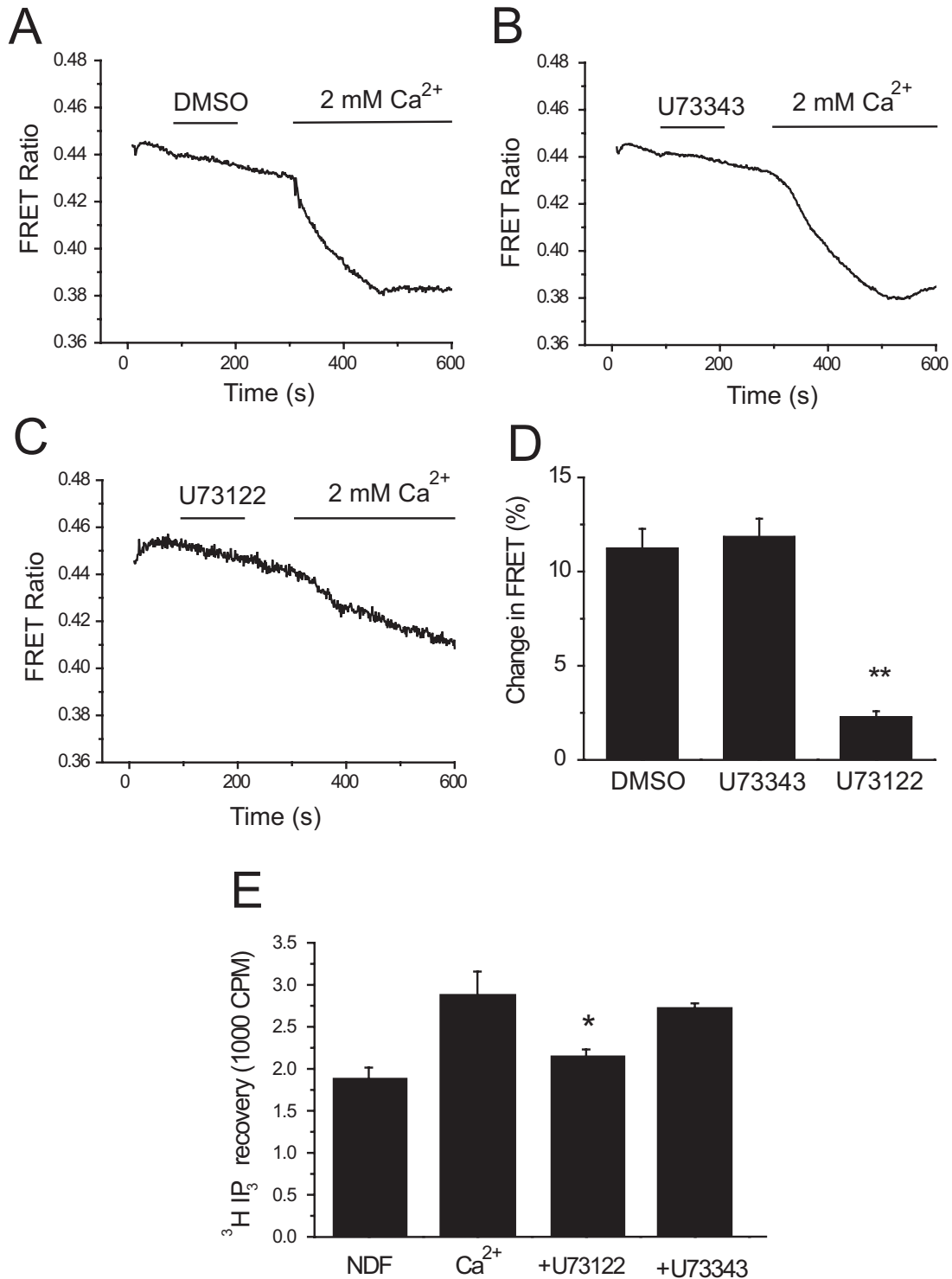

Fig. 3. U73122 inhibits Ca^{2+}-induced PIP_2 hydrolysis in TRPV6-expressing cells. Fluorescence was measured in HEK293 cells expressing TRPV6 and the CFP- and YFP-tagged PLCδ1 PH domains as described under *Materials and Methods*. Cells were kept in NDF solution for 20 min before the experiment. During the measurement, NDF was replaced with 2 mM Ca^{2+} to induce PIP_2 depletion. Cells were pretreated with DMSO (A), 3 μM U73343 (B), or 3 μM U73343 (C) for 2 min followed by a 2-min wash, and then 2 mM Ca^{2+} was added. The average change in FRET ratio ± S.E.M. was measured and plotted in D for DMSO ($n = 8$) U73343 ($n = 8$), or U73122 ($n = 10$) -treated cells. E, the effect of U73122 and U73343 on [^{3}H]IP_3 production, induced by 2 mM Ca^{2+}. Measurements were performed as described under Materials and Methods.

Discussion

Calcium transport in the intestines proceeds through both active transcellular and passive paracellular pathways. The transcellular process is driven energetically by the active extrusion of Ca^{2+} on the basolateral side of the duodenal epithelial cells both by the Ca^{2+} ATPase and the Na^+/Ca^{2+} exchanger. Ca^{2+} enters the cell, down its electrochemical gradient, from the lumen of the duodenum through the apical Ca^{2+} channel TRPV6 (Hoenderop et al., 2005; Christakos et al., 2007). High intracellular Ca^{2+} concentrations are toxic to cells; thus, these channels, similar to many other Ca^{2+} channels, inactivate when intracellular Ca^{2+} concentrations increase too high (Nilius et al., 2002; Derler et al., 2006; Thyagarajan et al., 2008). This inactivation is also likely to limit

intestinal Ca^{2+} absorption, although this notion has not yet been demonstrated experimentally. In the current study, we found that PLC inhibitors inhibit Ca^{2+}-induced inactivation of TRPV6 currents in heterologous expression systems. We also showed that inhibiting PLC enhances intestinal Ca^{2+} transport, suggesting that PLC activation and the ensuing TRPV6 inactivation limits intestinal Ca^{2+} transport.

In a previous study, we showed that Ca^{2+}-induced inactivation of TRPV6 is mediated by the depletion of PIP_2. That model is based on the following key observations (Thyagarajan et al., 2008). First, TRPV6 requires PIP_2 for activity in excised inside-out patches. Second, Ca^{2+}-induced inactivation could be prevented by dialyzing PIP_2 through the whole-cell patch pipette. Third, Ca^{2+} flowing through TRPV6 leads
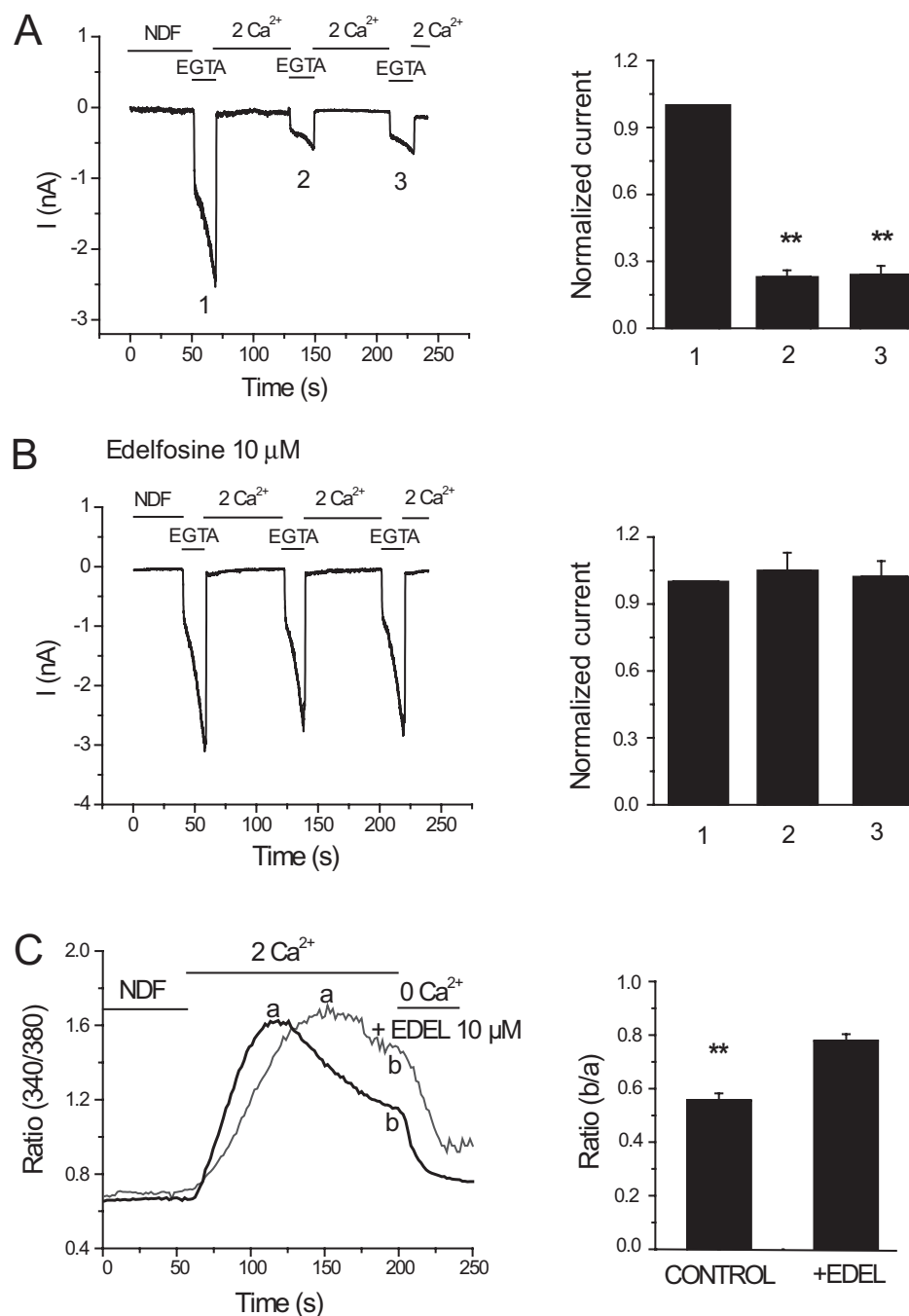

Fig. 4. Edelfosine inhibits Ca^{2+}-induced inactivation of TRPV6. Whole-cell patch-clamp recordings were performed as described in Fig. 1. Cells were preincubated for 20 min with vehicle (DMSO) or 10 μM edelfosine, which was also present during the measurements. A and B, left, time courses of monovalent currents through TRPV6 in control and edelfosine-treated cells, respectively. Right, mean $\pm$ S.E.M. of the currents remaining before the addition of 2 mM Ca^{2+}. The data were normalized to the peak current of the first 0 Ca^{2+} pulse (n = 8–9). C, left, time courses of Ca^{2+} entry into control and edelfosine (10 μM) preincubated cells. a and b, ratio values at the peak and 150 s after the addition of 2 mM Ca^{2+}. The fluorescence ratio values at b divided by the value at a are described on the right for the control and edelfosine-treated cells.

to depletion of PIP_2. Finally, selective depletion of PIP_2 using a chemically inducible PIP_2 phosphatase (Varnai et al., 2006) inhibited TRPV6.

In the present study, we focused on the role of PLC in Ca^{2+}-induced inactivation of TRPV6. The reasons for this are 2-fold. First, in principle, depletion of PIP_2 can happen in two different ways, via activation of PLC, where the end product is IP_3 and diacylglycerol, and via activation of a phosphatase, where the end product is PIP and inorganic phosphate. Both of these processes would inhibit TRPV6, because neither PIP nor diacylglycerol activates TRPV6. In the current study, we demonstrate conclusively that Ca^{2+}-induced PIP_2 depletion proceeds through activation of PLC. PIP_2 depletion, as measured by the translocation of the CFP- and YFP-tagged PH domains, was inhibited by both U73122 and edelfosine, but not the inactive U73343. In addition, we also show that Ca^{2+} flowing through TRPV6 induced formation of IP_3, which was blocked by U73122 but not by the inactive U73343.

Our second motivation to study the role of PLC was that this enzyme can be inhibited pharmacologically; thus, its role can be studied in a more physiological setting. In the expression system measurements, we tried three structurally different PLC inhibitors: U73122, edelfosine, and neomycin. U73122, the most widely used inhibitor of this enzyme, has a structurally very similar but inactive analog, U73343, which is often used as a negative control (Balla, 2001). One of the side effects of U73122 is that upon prolonged exposure, it also depletes PIP_2, presumably because it is also a partial activator of PLC (Horowitz et al., 2005). In experiments in which the goal of inhibiting PLC is to prevent the formation of IP_3, this is not necessarily a problematic side effect; both inhibition of PLC and depletion of PIP_2 will lead to diminished formation of IP_3. In experiments in which the goal is to

prevent the depletion of PIP_2, this effect can offset the inhibitory effect on PLC. This problem was addressed by Horowitz et al. (2005), who thoroughly measured the time- and concentration-dependence of both the PLC inhibitory and PIP_2 depletion-inducing effects of U73122. They found that a brief pretreatment with relatively high concentration (3 μM) of U73122, followed by the removal of the agent, minimizes the PIP_2-depleting effect yet leaves the inhibitory effect on PLC intact for the time scale of the patch-clamp/fluorescence experiments (~10 min). Later, we also used a similar protocol to study the role of PLC in desensitization of TRPV1 currents (Lukacs et al., 2007). In the current study, U73122, but not its inactive analog U73343, inhibited PLC activation and Ca^{2+}-induced inactivation of TRPV6.

Horwitz et al. also introduced another PLC inhibitor, edelfosine (ET-18-OCH3), which does not suffer from these uncertainties, it does not deplete PIP_2, and it can be left in the experimental media during the experiments. In our hands, edelfosine also inhibited Ca^{2+}-induced PIP_2 depletion and Ca^{2+}-induced inactivation of TRPV6 in cellular experiments. The intestinal Ca^{2+} transport measurements are performed on a different time scale (1 h) and on a whole organ preparation; thus, it is likely that the treatment protocols with U73122 from the cellular measurements cannot be directly applied to these experiments. Because both PIP_2 depletion and waning of the effect of U73122 during the 1-h Ca^{2+} transport measurement could be a problem, we decided to use edelfosine to inhibit PLC in these experiments. Edelfosine enhanced duodenal Ca^{2+} transport, as can be expected if Ca^{2+}-induced inactivation mediated by PLC activation limits intestinal Ca^{2+} transport.

Another widely used PLC inhibitor is neomycin. This compound is believed to block PLC by chelating its substrate,
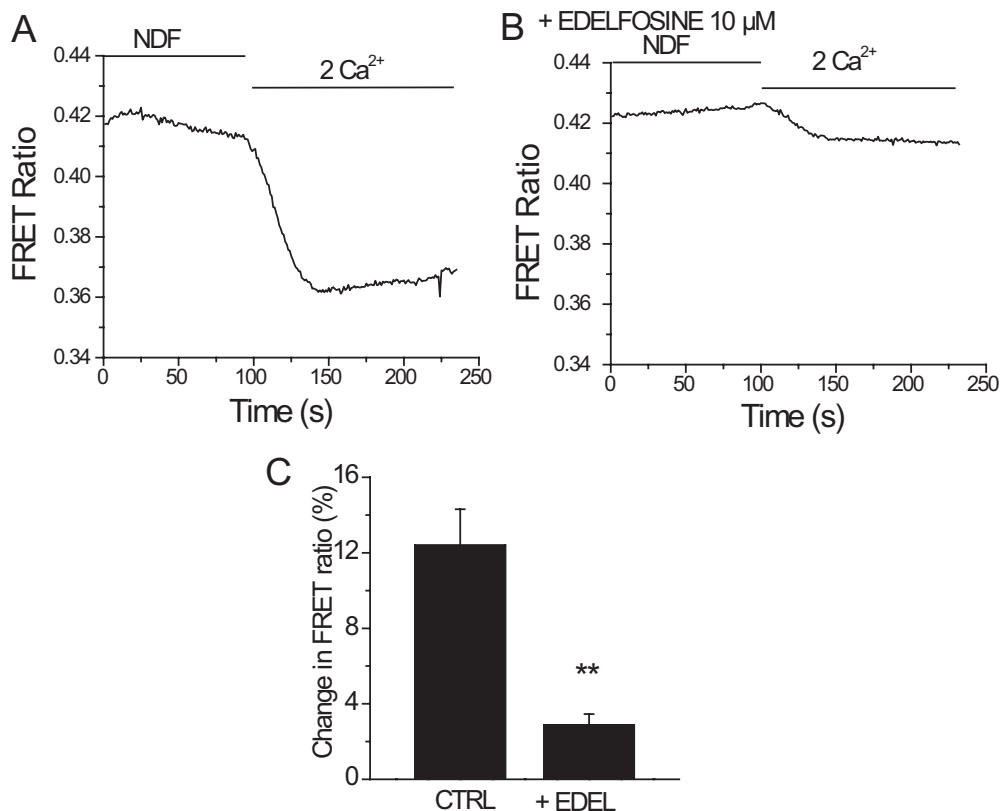

Fig. 5. Edelfosine inhibits Ca^{2+}-induced PIP_2 hydrolysis. Fluorescence was measured in HEK293 cells expressing TRPV6 and the CFP- and YFP-tagged PLCδ1 PH domains as described under *Materials and Methods*. Time courses of changes in FRET ratio induced by addition of 2 mM Ca^{2+} in cells expressing TRPV6 pretreated with DMSO (A) or 10 μM edelfosine (B). The average change in FRET ratio $\pm$ S.E.M. was measured and plotted in C for DMSO- ($n = 8$) or edelfosine ($n = 13$)-treated cells.

PIP$_2$ (Gabev et al., 1989). Again, in experiments in which the goal is to prevent the formation of IP$_3$, this mechanism can produce meaningful results. In our setting, however, in which the goal is to prevent PIP$_2$ depletion this is not a desirable mechanism of action. In accordance with this note, neomycin strongly inhibited TRPV6 currents in our hands; thus, we could not use this inhibitor to study Ca^{2+}-induced inactivation of the channel.

The data in this article together with our previous data (Thyagarajan et al., 2008) delineate a mechanism in which Ca^{2+} flowing through TRPV6 activates a Ca^{2+}-sensitive PLC, and the resulting depletion of PIP$_2$ limits channel activity. It is noteworthy that this or a similar mechanism has been proposed to mediate the inactivation/desensitization of several other TRP channels (Rohacs and Nilius, 2007), including TRPM8 (Rohacs et al., 2005), TRPV1 (Liu et al., 2005; Lishko et al., 2007; Lukacs et al., 2007), and TRPM4 (Nilius et al., 2006).

The prototypical Ca^{2+} sensor calmodulin has also been implicated in Ca^{2+}-induced inactivation of TRPV6 (Niemeyer et al., 2001; Derler et al., 2006). Those studies have been performed with higher extracellular [Ca^{2+}] (10–30 mM) and on a much shorter time scale (several hundred milliseconds). It will require further studies to elucidate the roles of calmodulin and PIP$_2$ depletion and their potential interplay in inactivation of TRPV6. It has to be noted that one article described positive regulation of TRPV6 by calmodulin (Lambers et al., 2004).

In conclusion, our study demonstrates the role of PLC in Ca^{2+}-induced inactivation of TRPV6. According to our model, Ca^{2+} flowing through TRPV6 activates a Ca^{2+}-sensitive PLC, and the ensuing depletion of PIP$_2$ limits channel activity, contributing to inactivation of the channels. We show that two structurally different compounds inhibit both PLC activation and Ca^{2+}-induced inactivation of TRPV6. We also show that pharmacological inhibition of PLC enhances intestinal Ca^{2+} transport. This raises the possibility that pharmacological tools targeting PLC can be used to enhance intestinal Ca^{2+} absorption. Given the prevalence of osteoporosis, which generally comes with negative Ca^{2+} balance, PLC can be a clinically relevant pharmacological target in the future.
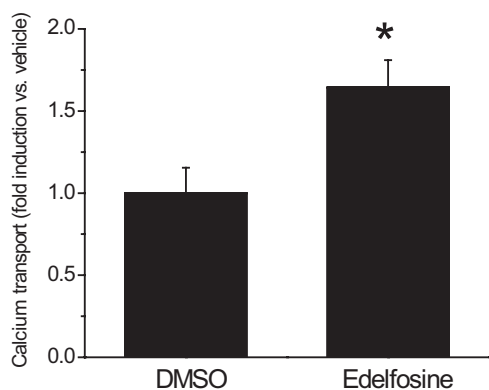

Fig. 6. Edelfosine enhances intestinal Ca^{2+} transport. ^{45}Ca uptake of everted duodenal sacs was measured as described under *Materials and Methods*. Duodenal sacs were pretreated with DMSO or 10 μM edelfosine for 20 min, the vehicle or edelfosine was present throughout the 1-h transport measurement. Edelfosine significantly enhanced ^{45}Ca transport, $n = 7$ for DMSO and $n = 9$ for edelfosine, $p < 0.05$.

References

Balla T (2001) Pharmacology of phosphoinositides, regulators of multiple cellular functions. *Curr Pharm Des* **7:**475–507.

Benn BS, Ajibade D, Porta A, Dhawan P, Hediger M, Peng JB, Jiang Y, Oh GT, Jeung EB, Lieben L, et al. (2008) Active intestinal calcium transport in the absence of TRPV6 and calbindin-D9k. *Endocrinology* **149:**3196–3205.

Bianco SD, Peng JB, Takanaga H, Suzuki Y, Crescenzi A, Kos CH, Zhuang L, Freeman MR, Gouveia CH, Wu J, et al. (2006) Marked disturbance of calcium homeostasis in mice with targeted disruption of the Trpv6 calcium channel gene. *J Bone Miner Res* **22:**274–285.

Christakos S, Dhawan P, Benn B, Porta A, Hediger M, Oh GT, Jeung EB, Zhong Y, Ajibade D, Dhawan K, et al. (2007) Vitamin D: molecular mechanism of action. *Ann N Y Acad Sci* **1116:**340–348.

Christakos S, Dhawan P, Liu Y, Peng X, and Porta A (2003) New insights into the mechanisms of vitamin D action. *J Cell Biochem* **88:**695–705.

Clapham DE, Runnels LW, and Strübing C (2001) The TRP ion channel family. *Nat Rev Neurosci* **2:**387–396.

Cui J, Bian JS, Kagan A, and McDonald TV (2002) CaT1 contributes to the stores-operated calcium current in Jurkat T-lymphocytes. *J Biol Chem* **277:**47175–47183.

den Dekker E, Hoenderop JG, Nilius B, and Bindels RJ (2003) The epithelial calcium channels, TRPV5 & TRPV6: from identification towards regulation. *Cell Calcium* **33:**497–507.

Derler I, Hofbauer M, Kahr H, Fritsch R, Muik M, Kepplinger K, Hack ME, Moritz S, Schindl R, Groschner K, et al. (2006) Dynamic but not constitutive association of calmodulin with rat TRPV6 channels enables fine tuning of Ca^{2+}-dependent inactivation. *J Physiol* **577:**31–44.

Gabev E, Kasianowicz J, Abbott T, and McLaughlin S (1989) Binding of neomycin to phosphatidylinositol 4,5-bisphosphate (PIP$_2$). *Biochim Biophys Acta* **979:**105–112.

Hardie RC (2003) Regulation of TRP channels via lipid second messengers. *Annu Rev Physiol* **65:**735–759.

Hirose K, Kadowaki S, Tanabe M, Takeshima H, and Iino M (1999) Spatiotemporal dynamics of inositol 1,4,5-trisphosphate that underlies complex Ca^{2+} mobilization patterns. *Science* **284:**1527–1530.

Hoenderop JG, Nilius B, and Bindels RJ (2005) Calcium absorption across epithelia. *Physiol Rev* **85:**373–422.

Hoenderop JG, van Leeuwen JP, van der Eerden BC, Kersten FF, van der Kemp AW, Mérillat AM, Waarsing JH, Rossier BC, Vallon V, Hummler E, et al. (2003) Renal Ca^{2+} wasting, hyperabsorption, and reduced bone thickness in mice lacking TRPV5. *J Clin Invest* **112:**1906–1914.

Horowitz LF, Hirdes W, Suh BC, Hilgemann DW, Mackie K, and Hille B (2005) Phospholipase C in living cells: activation, inhibition, Ca^{2+} requirement, and regulation of M current. *J Gen Physiol* **126:**243–262.

Lambers TT, Weidema AF, Nilius B, Hoenderop JG, and Bindels RJ (2004) Regulation of the mouse epithelial Ca^{2+} channel TRPV6 by the Ca^{2+}-sensor calmodulin. *J Biol Chem* **279:**28855–28861.

Lishko PV, Procko E, Jin X, Phelps CB, and Gaudet R (2007) The ankyrin repeats of TRPV1 bind multiple ligands and modulate channel sensitivity. *Neuron* **54:**905–918.

Liu B, Zhang C, and Qin F (2005) Functional recovery from desensitization of vanilloid receptor TRPV1 requires resynthesis of phosphatidylinositol 4,5-bisphosphate. *J Neurosci* **25:**4835–4843.

Lukacs V, Thyagarajan B, Varnai P, Balla A, Balla T, and Rohacs T (2007) Dual regulation of TRPV1 by phosphoinositides. *J Neurosci* **27:**7070–7080.

Niemeyer BA, Bergs C, Wissenbach U, Flockerzi V, and Trost C (2001) Competitive regulation of CaT-like-mediated Ca^{2+} entry by protein kinase C and calmodulin. *Proc Natl Acad Sci U S A* **98:**3600–3605.

Nilius B, Mahieu F, Prenen J, Janssens A, Owsianik G, Vennekens R, and Voets T (2006) The Ca^{2+}-activated cation channel TRPM4 is regulated by phosphatidylinositol 4,5-biphosphate. *EMBO J* **25:**467–478.

Nilius B, Prenen J, Hoenderop JG, Vennekens R, Hoefs S, Weidema AF, Droogmans G, and Bindels RJ (2002) Fast and slow inactivation kinetics of the Ca^{2+} channels ECaC1 and ECaC2 (TRPV5 and TRPV6). Role of the intracellular loop located between transmembrane segments 2 and 3. *J Biol Chem* **277:**30852–30858.

Nilius B, Prenen J, Vennekens R, Hoenderop JG, Bindels RJ, and Droogmans G (2001) Modulation of the epithelial calcium channel, ECaC, by intracellular Ca^{2+}. *Cell Calcium* **29:**417–428.

Peng JB, Chen XZ, Berger UV, Vassilev PM, Tsukaguchi H, Brown EM, and Hediger MA (1999) Molecular cloning and characterization of a channel-like transporter mediating intestinal calcium absorption. *J Biol Chem* **274:**22739–22746.

Rohács T, Lopes CM, Michailidis I, and Logothetis DE (2005) PI(4,5)$_2$ Regulates the activation and desensitization of TRPM8 channels through the TRP domain. *Nat Neurosci* **8:**626–634.

Rohacs T and Nilius B (2007) Regulation of transient receptor potential (TRP) channels by phosphoinositides. *Pflugers Arch* **455:**157–168.

Runnels LW, Yue L, and Clapham DE (2002) The TRPM7 channel is inactivated by PIP$_2$ hydrolysis. *Nat Cell Biol* **4:**329–336.

Suh BC, Inoue T, Meyer T, and Hille B (2006) Rapid chemically induced changes of PtdIns(4,5)P$_2$ gate KCNQ ion channels. *Science* **314:**1454–1457.

Thyagarajan B, Lukacs V, and Rohacs T (2008) Hydrolysis of phosphatidylinositol 4,5-bisphosphate mediates calcium induced inactivation of TRPV6 channels. *J Biol Chem* **283:**14980–14987.

van der Wal J, Habets R, Várnai P, Balla T, and Jalink K (2001) Monitoring agonist-induced phospholipase C activation in live cells by fluorescence resonance energy transfer. *J Biol Chem* **276:**15337–15344.

Varnai P, Thyagarajan B, Rohacs T, and Balla T (2006) Rapidly inducible changes in phosphatidylinositol 4,5-bisphosphate levels influence multiple regulatory functions of the lipid in intact cells. *J Cell Biol* **175:**377–382.

Voets T and Nilius B (2007) Modulation of TRPs by PIPs. *J Physiol* **582:**939–944.

Wasserman RH (2004) Vitamin D and the intestinal absorption of calcium: a view and overview, in *Vitamin D* (Feldman D, Pike JW, and Glorieux F eds) 411–428, Academic Press.

Zhang Z, Okawa H, Wang Y, and Liman ER (2005) Phosphatidylinositol 4,5-bisphosphate rescues TRPM4 channels from desensitization. *J Biol Chem* **280:**39185–39192.

Address correspondence to: Dr. Tibor Rohacs, Department of Pharmacology and Physiology, University of Medicine and Dentistry of New Jersey, New Jersey Medical School, 185 South Orange Avenue, Newark, NJ 07103. E-mail: tibor.rohacs@umdnj.edu